Pass 7. An upgrade to Fermi-LAT analysis

Markus Ackermann, Bill Atwood & Riccardo Rando
on behalf of the Fermi LAT collaboration

Abstract: To date the LAT data have been analyzed using an event-level analysis scheme developed before launch, denoted Pass 6. Not surprisingly, the real flight data had unanticipated features which needed to be accommodated. This was done via after-the-fact patches to the analyzed data. Pass 7, which is about to be released, is the first re-work of the LAT event-level analysis in which these observed effects were both incorporated in the simulations and used to develop and optimize photon event selection and charged particle background rejection criteria. In addition, the utilization of the preconceived event classes has been reassessed to conform to the current usage both within the LAT collaboration and the user community. We describe here the changes made to the simulated data used to develop the event level analysis as well as the modifications and additions to the event classes. The checks of the Pass 7 reprocessing using real data are also summarized.

Simulation update & Monte Carlo based multivariate event selection

Modifications to the simulation

The most significant omission in the simulations of the operational LAT on-orbit was the failure to include effects due to the finite-time signals persisting in the electronics [1,2]. For the three main LAT particle detection subsystems, perhaps the most notable was the Tracker in which signals last ~ 10 μs after the passage of a charged particle. This leads to the overlap of cosmic rays (CRs) within gamma-ray events. These out-of-time CRs were named "ghost tracks". The level of this contamination varies according to the trigger rate and is between 4% and 14%. Events with ghosts are mostly eliminated as background and hence cause an unaccounted for inefficiency in the background rejection.

In order to capture this phenomenon simulated gamma-ray events were overlaid on top of real events from the LAT taken with a periodic trigger. This not only serves to capture the ghost event phenomena, but also provided an accurate account of any noise sources. A typical overlaid gamma-ray event is shown below.

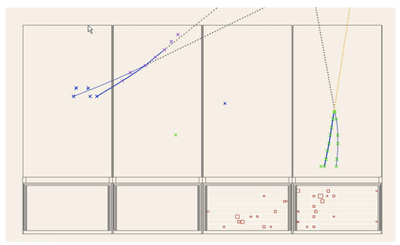

A one-event display showing a simulated gamma-ray event (on the right) with a periodic trigger event overlaid on it. The various lines indicate Tracker reconstructions both from the ground processing as well as what was done on-board in orbit.

It should be recognized here that the event reconstruction algorithms were not modified for Pass 7; that major effort was deferred to the subsequent Pass 8 still in development (see dedicated poster [3]).

The three LAT particle detection sub-systems

Anti-Coincidence Detector: Minimize contamination from entering charged CR

Tracker: Identify photon-like topologies and track types via detailed hit analysis

Calorimeter: Identify electromagnetic shower energy depositions

In the background analysis, each subsystem is analyzed separately and then these separate analyses are combined to provide various levels of background rejection in exchange for effective area. The subsystem analyses contain two parts: cuts to eliminate specific sources of background and obvious categories of background events followed by the evaluation of the probability, generated by a classification tree ensemble (CT), that the event was a gamma ray. The CT step allowed for up to an order-of-magnitude increase in rejection albeit at the expense of the effective area.

Anti-Coincidence Detector (ACD)

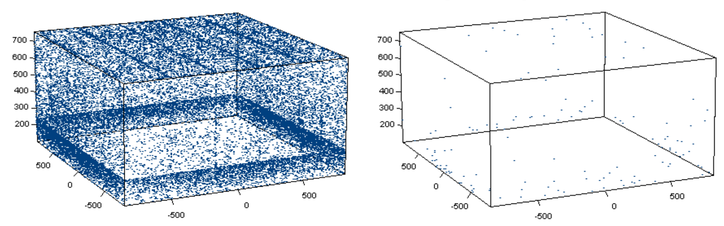

The left-hand plot shows the entry points of CR from the simulations which both trigger the LAT and pass the onboard analysis. The obvious patterns reflect the structure of the ACD (gaps on the top and limitation of side coverage). The right hand plot shows the remaining events after the cuts and a modest cut on the ACD CT probability (> .20).

Tracker & Calorimeter

For events which remain after the ACD analysis, the effectiveness of the Tracker and Calorimeter are characterized by a set of cuts followed by a CT probability. How these play out is shown to the left in 4 decades of energy from 18 MeV to 180 GeV. CRs are shown in red, gamma rays in blue.

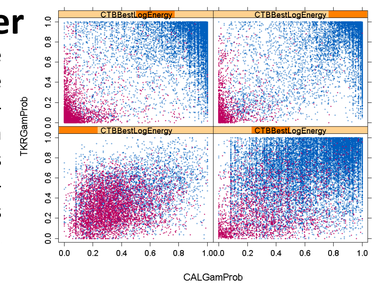

Combining subsystems

The CT probabilities for the Tracker and Calorimeter along with a handful of other cross-system variables are used as input to a final CT analysis. The resulting overall probability is shown below first as the probability distributions for gamma rays and CRs, and then used as the independent parameter to map out a contour in the space of CR background rate versus gamma-ray efficiency.

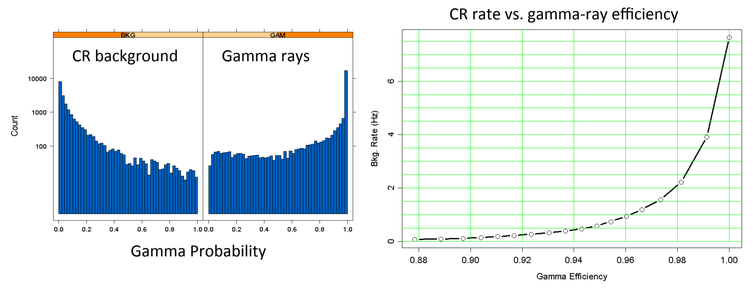

Event sample definition & verification on flight data

Pass 7 event classes

Stringent background rejection implies some unavoidable loss of effective area of the detector. As in the Pass 6 event classification we therefore define several event classes to suit different analysis needs. The table below summarizes the new standard event classes.

Less CR background ↓ / ↑ More effective area

Event class	Purpose	Pass 6 equivalent
P7TRANSIENT	Analysis of short transients (GRBs, Flares)	*P6_v3_transient* (class ≥1 events)
P7SOURCE	2nd LAT catalog, analysis of point sources	*P6_v3_diffuse* (class ≥3 events)
P7CLEAN	Study of extended sources & diffuse gamma-ray emission	*P6_v3_dataclean* (class 4 events)
P7ULTRACLEAN	Analysis of the extra-galactic gamma-ray background	None

Flight data verification for event classes

The definition of the standard event classes beyond the transient class was developed with the help of a detailed comparison of the output of the multivariate classification analysis to that of the flight data. Data from a photon-rich region of the sky (direction of the Galactic ridge) and a photon-poor region (high Galactic latitude) are compared to the simulation to design energy dependent selection criteria on the classification analysis output. Furthermore the data were scanned for potential backgrounds not removed in the classification analysis and additional selection criteria were devised to reject such backgrounds.

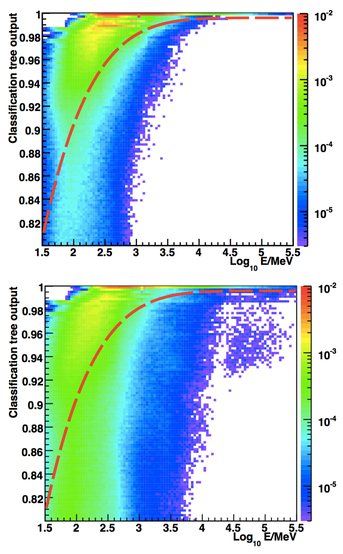

Distribution of the main output variable of the multivariate event classification analysis as a function of photon energy. The upper plot shows the distribution for the data sample from a photon-rich region of the sky (low background), the lower plot shows the data sample from a photon-poor region of the sky (high background). Both distributions are normalized. The red dashed line indicates the event selection criterion used for the definition of the P7SOURCE event class. Only events above the red line are retained in the 'source' class sample.

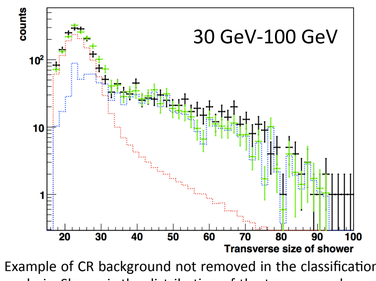

Example of CR background not removed in the classification analysis. Shown is the distribution of the transverse shower size for events from the photon-poor region of the sky (black). The expected distributions for gamma-rays (red), CR background (blue) and their sum (green) are indicated. The transverse shower size is used as a selection criterion to define the P7CLEAN and P7ULTRACLEAN event classes.

Residual background estimation

We estimate the residual background from a large production of CR background. Primary protons and electrons are simulated isotropically. Back-tracing of the particle trajectories through the geomagnetic field is used to reject trajectories shadowed by the Earth. The secondary cosmic-ray component is simulated according to the LAT background model.

A comparison between the simulated and real data of several key variables used in the event selection shows agreement between observed and predicted background rates at the ±50% level.

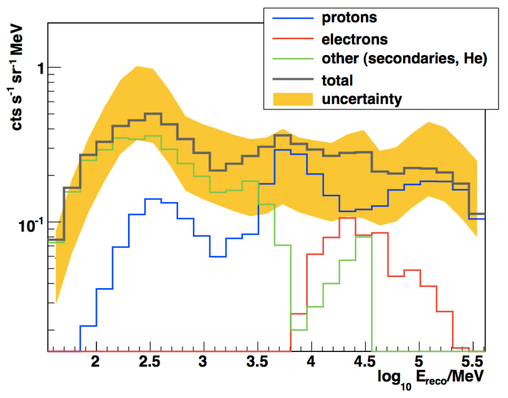

Average rate of CR-induced background between 30 MeV and 300 GeV in the P7SOURCE event class. The dotted line shows the total CR background predicted by the simulation. The yellow band depicts the uncertainty range for the observed cosmic ray background. The uncertainty estimate is obtained by rescaling the simulation prediction to the observed distributions for several variables used in the event selection.

Instrument response functions & performance

Instrument response functions for Pass 7 science

The IRFs give a parametric description of the LAT performance in terms of efficiency (*effective area*), angular resolution (*point spread function*) and energy resolution (*energy dispersion*).

In addition to the improved performance of the Pass 7 analysis we have improved our IRFs by adding the capability of describing some second-order effects. The effective area now includes a description of the dependence of efficiency on the azimuthal angle (*phi-dependence*) around the LAT boresight. This is a small effect (a few percent) due to the LAT mechanical structure: gaps are always aligned along x and y axes. The clearest effect of phi-dependence is a fractional variability of bright sources (e.g. Vela) over short time scales as the relative exposure at different phi values varies. Accounting for phi dependence in source analysis is not routinely done, as over long time periods the dependence on phi can be expected to nearly average for most point sources.

Since P6_v3 IRFs, the effective area is evaluated taking into account considerations related to pile-up effects due to the high background rates in orbit, averaged over long timescales. We now provide a description of the variation over short timescales (a few percent) due to the different sampling of geomagnetic coordinates along the LAT orbit, exploiting the correlation of particle background rates and LAT livetime fraction. *Livetime dependence* is accounted for automatically when using P7_V6 IRFs. Further details about IRF validation can be found on a dedicated poster [4].

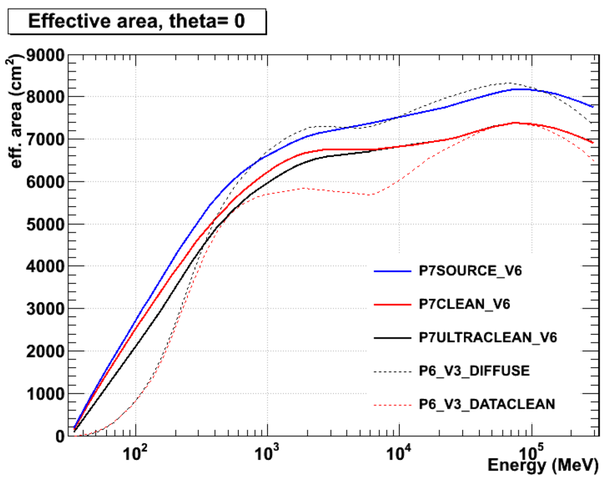

Normal incidence effective area for Pass 7 P7_V6 IRFs (solid thick lines). The same quantities for P6_V3 IRFs are superimposed (thin dotted lines). Effective area values are averaged over all phi values and over geomagnetic history. Smoothing is applied.

The gain in the effective area at low energies is evident. The improved treatment of the various sources of systematics makes it possible to use the low end of the LAT energy acceptance down to ~ 50 MeV. At high energy P7SOURCE class is comparable to the old P6_V3_DIFFUSE class, but known sources of systematics were addressed, so the confidence is actually greater. The clean classes, derived as detailed above, have superior performance with respect the older P6_V3_DATACLEAN.

A careful analysis is currently ongoing to numerically evaluate all the different sources of systematics that can impact on the reconstructed spectrum of a source, and results will become public soon. In a dedicated paper we will provide an exhaustive description of the LAT event analysis, of the performance parametrization, and of the procedures we have developed for the assessment of systematics.

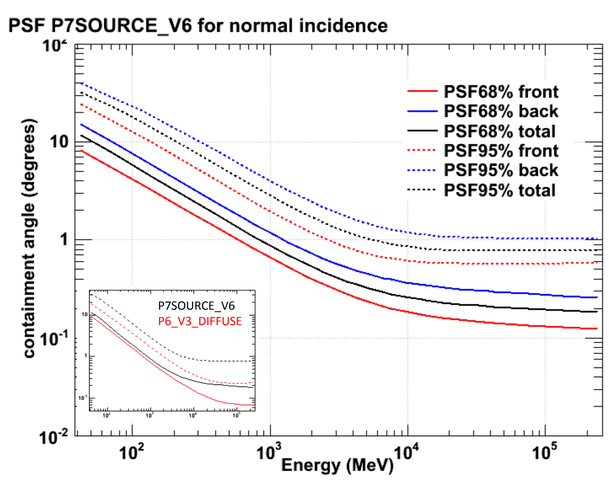

Point Spread Function (PSF) for P7SOURCE_V6 IRFs; the PSF for the other P7 clean classes is hardly distinguishable from this; in the caption: comparison of 68% and 95% containment between older P6_V3_DIFFUSE psf and P7SOURCE_V6.

PSF above 1 GeV is derived from on-orbit data to address the known discrepancy between the estimates based on Monte Carlo and the values we derive from analysis of point sources in this energy range. The in-flight PSF is based on a dedicated likelihood analysis that derives the angular containment from a study of photon distribution around bright pulsars (1-10 GeV) and a selected sample of bright AGN (>10 GeV) [5]. The resulting PSF parameters are smoothed within statistical uncertainties and seamlessly connected with the Monte Carlo based values at 1 GeV. At the highest energies the angular resolution we derive is worse than the Monte Carlo estimate by a factor 2 to 3, while at 1 GeV no significant discrepancy is observed. Systematics are being carefully evaluated and will be described in a dedicated paper.

References:

[1] Atwood, W. B. et al., "*The Large Area Telescope on the Fermi Gamma-ray Space Telescope Mission*", ApJ, 697, 1071 (2009)
[2] R. Rando, "*Post-launch performance of the Fermi Large Area Telescope*", arXiv:0907.0626v1, 2009
[3] Baldini L. for the Pass-8 group, *"Pass 8: A comprehensive revision of the Fermi LAT event-level analysis."*, this conference
[4] Charles E. et al., *"Validation and Calibration of the Large Area Telescope Effective Area Using Two Years of Flight Data"*, this conference
[5] Roth M. et al., "*On-orbit Determination of the LAT Point Spread Function*", this conference